HHS Public Access

Author manuscript

Immunity. Author manuscript; available in PMC 2016 October 20.

Published in final edited form as:

Immunity. 2015 October 20; 43(4): 703–714. doi:10.1016/j.immuni.2015.09.002.

T follicular helper cell-dependent clearance of a persistent virus infection requires T cell expression of the histone demethylase UTX

Kevin D. Cook[1,7], **Karl B. Shpargel**[1,2,3,7], **Joshua Starmer**[1,2,3], **Fatima Whitfield-Larry**[4,5], **Bridget Conley**[4], **Denise E. Allard**[5], **Julia E. Rager**[6], **Rebecca C. Fry**[6], **Marsha L. Davenport**[4], **Terry Magnuson**[1,2,3], **Jason K. Whitmire**[1,5,8,*], and **Maureen A. Su**[4,5,8,*]

[1] Department of Genetics, University of North Carolina at Chapel Hill School of Medicine, 120 Mason Farm Road, Chapel Hill, NC, 27599, USA.

[2] Carolina Center for Genome Sciences, University of North Carolina at Chapel Hill School of Medicine, 120 Mason Farm Road, Chapel Hill, NC, 27599, USA.

[3] Lineberger Comprehensive Cancer Center, University of North Carolina at Chapel Hill School of Medicine, 120 Mason Farm Road, Chapel Hill, NC, 27599, USA.

[4] Department of Pediatrics, University of North Carolina at Chapel Hill School of Medicine, 120 Mason Farm Road, Chapel Hill, NC, 27599, USA.

[5] Department of Microbiology and Immunology, University of North Carolina at Chapel Hill School of Medicine, 120 Mason Farm Road, Chapel Hill, NC, 27599, USA.

[6] Department of Environmental Sciences and Engineering, University of North Carolina at Chapel Hill School of Medicine, 120 Mason Farm Road, Chapel Hill, NC, 27599, USA.

Summary

Epigenetic changes, including histone methylation, control T cell differentiation and memory formation, though the enzymes that mediate these processes are not clear. We show that UTX, a histone H3 lysine 27 (H3K27) demethylase, supports T follicular helper (Tfh) cell responses that are essential for B cell antibody generation and the resolution of chronic viral infections. Mice with a T cell-specific UTX deletion had fewer Tfh cells, reduced germinal center responses, lacked virus-specific IgG, and were unable to resolve chronic lymphocytic choriomeningitis virus

* Correspondence: Maureen Su (masu@email.unc.edu); Jason Whitmire (jwhitmir@email.unc.edu).
[7] Co-first author
[8] Co-senior author

Author Contributions

KDC and KBS (equal contribution) performed experiments, analyzed data, and wrote the manuscript. JS performed data analysis and contributed to writing the manuscript. FWL, BC, and DEA performed experiments. JER, and RCF performed data analysis. MLD assisted with patient sample collection and analyzed data. TM was involved in study design. JKW and MAS (equal contribution) designed these studies, analyzed the data, supervised the projects, and wrote the manuscript.

The authors have no conflicts of interest to declare.

infections. UTX-deficient T cells showed decreased expression of interleukin-6 receptor-α and other Tfh cell-related genes that were associated with increased H3K27 methylation. Additionally, Turner Syndrome subjects, who are predisposed to chronic ear infections, had reduced UTX expression in immune cells and decreased circulating $CD4^+$ $CXCR5^+$ T cell frequency. Thus, we identify a critical link between UTX in T cells and immunity to infection.

Graphical Abstract

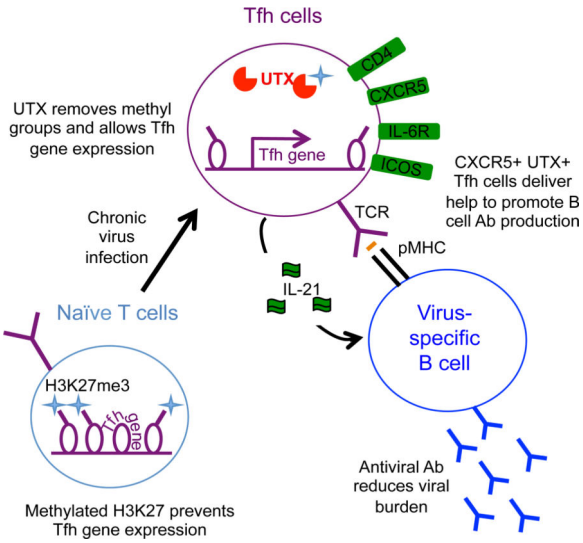

Introduction

Hundreds of millions of people worldwide are infected with viruses that persist and induce devastating diseases (Virgin et al., 2009). Viruses such as HIV, HCV, and HBV establish chronic infections when the adaptive immune response initially fails to eliminate them. Over time, extended exposure to viral antigens and sustained inflammation further diminishes the T cell response. In contrast to acute infections, where highly functional memory T cells form following transient expansion and contraction phases, chronic infections lead to virus specific $CD8^+$ T cell exhaustion, in which cells are physically depleted or functionally inactivated (Wherry, 2011). Overcoming T cell exhaustion in persistent viral infection is a potential approach to enhance the antiviral immune response.

$CD4^+$ T cells support $CD8^+$ T cell responses and preferentially differentiate into the T follicular helper (Tfh) cell subset during chronic viral infections (Brooks et al., 2005; Fahey et al., 2011; Matloubian et al., 1994; Thomsen et al., 1996). This increase in Tfh cell differentiation is enhanced by the repetitive T cell receptor (TCR) activation that occurs during persistent infection (Fahey et al., 2011). As a result, increased populations of virus-specific Tfh cells are observed during chronic lymphocytic choriomeningitis virus (LCMV) infection of mice, as well as HIV, HBV, and HCV infections of humans (Fahey et al., 2011; Feng et al., 2012; Feng et al., 2011; Lindqvist et al., 2012). Tfh cells upregulate CXCR5, which enables them to relocate to B cell areas of lymphoid organs. Tfh cells interact with B cells to generate plasmablasts or enter germinal centers (GCs) to drive B cell proliferation,

antibody affinity maturation, isotype class switching, and the formation of memory B cells and plasma cells (Crotty, 2011). The shift toward $CD4^+$ Tfh cell differentiation is functionally important because B cells and antibody production are crucial for eventual virus control in mouse models of chronic infection (Bergthaler et al., 2009; Planz et al., 1997). $CD4^+$ Tfh cells also produce IL-21, a cytokine that sustains $CD8^+$ T cells during chronic viral infections (Elsaesser et al., 2009; Frohlich et al., 2009; Yi et al., 2009). The importance of Tfh cells may be conserved in humans, as a distinct population of circulating memory Tfh cells correlates with broadly neutralizing antibodies against HIV (Locci et al., 2013). Although IL-6 production by follicular dendritic cells is required for Tfh cell responses and control of chronic LCMV infection (Harker et al., 2011), how virus persistence advances Tfh differentiation is not understood.

The differentiation of $CD4^+$ T helper (Th) cells into distinct lineages correlates with specific epigenetic modifications (Wei et al., 2009; Wilson et al., 2009). These epigenetic changes include post-translational histone methylation, which modulate nucleosome structure to regulate transcription factor accessibility. For example, H3K27me3 contributes to repressive chromatin and gene silencing, while histone H3 lysine 4 trimethylation (H3K4me3) is indicative of genes that are actively transcribed (Bannister and Kouzarides, 2011). The H3K27 methyltransferase Enhancer of Zeste Homolog 2 (EZH2) regulates Th1 and Th2 differentiation, and EZH2 deficiency enhances interferon gamma (IFN-γ) and IL-4 production *in vitro* and allergic asthma pathology *in vivo* (Tumes et al., 2013). In these models, EZH2-mediated trimethylation of H3K27 represses gene expression and restricts the differentiation of Th progenitor cells. However, which histone demethylases promote Th lineage differentiation *in vivo* is not known.

UTX (ubiquitously transcribed tetratricopeptide repeat, X chromosome; KDM6A), along with UTY and JMJD3 (KDM6B), are members of an evolutionarily conserved, Jumonji-C (JmjC) domain containing family of H3K27me3 demethylases (Agger et al., 2007). *Utx* is widely expressed and has functions in biological processes ranging from embryonic development to tumor suppression, and homozygous *Utx* mutations in the mouse are embryonic lethal (Shpargel et al., 2012). In this study, we generated T cell-specific UTX-deficient (UTX-TCD) mice to assess the *in vivo* effects of UTX on T cell activation and differentiation during acute and chronic virus infection. Our results indicate that UTX is required for optimal $CD4^+$ T cell differentiation to Tfh cells during chronic, but not acute, virus infection. Moreover, UTX-TCD mice showed defects in germinal center formation, virus-specific IgG production, and clearance of a chronic viral infection. UTX deficiency resulted in increased H3K27 methylation and decreased expression at *Il6ra* and other Tfh-related genetic loci. Furthermore, human Turner Syndrome subjects with decreased UTX expression in peripheral blood also demonstrated decreased numbers of circulating $CD4^+$ $CXCR5^+$ T cells. These results delineate a link between a histone demethylase in T cells and immunity to chronic virus infection.

Results

Lack of T cell UTX does not alter clearance of acute viral infection

To study the role of UTX in T cells, we generated T cell-specific UTX-deficient mice by crossing the *Utx*^{fl} line, which harbors a floxed third exon, with mice expressing Cre recombinase under the control of the T cell-specific *Lck* promoter. Females with a Cre-mediated *Utx* deletion in T cells (*Utx*$^{fl/fl}$*; Lck-Cre*), hereafter referred to as UTX-TCD (T cell deficient), were born at expected frequencies and matured to adulthood. A T cell-specific decrease of UTX protein was confirmed by western blotting of sorted splenocytes from UTX-TCD mice relative to *Utx*$^{fl/fl}$ controls (referred to as WT) (Figure S1A). We first evaluated the role of UTX in T cell thymic development and peripheral maintenance under homeostatic conditions. In 6 week-old UTX-TCD mice, CD4^{+} and CD8^{+} T cell development was unchanged in the thymus, while modest decreases in CD4^{+} and CD8^{+} T cell frequencies and numbers were noted in the spleen (Figure S1B,C). Given the modest decrease in peripheral CD4^{+} and CD8^{+} T cells, we assessed the proliferative capacity of UTX-deficient T cells by stimulating CFSE-labeled splenocytes with plate-bound anti-CD3 and anti-CD28 antibodies. We detected equivalent cell division between WT and UTX-TCD CD4^{+} and CD8^{+} T cells across a range of anti-CD3 concentrations (Figure S1D). Thus, the T cell-specific deletion of UTX results in moderate decreases in CD4^{+} and CD8^{+} T cell numbers without affecting their proliferative response to *in vitro* TCR stimulation.

To assess the functional consequence of T cell UTX deficiency during an *in vivo* immune response, we infected UTX-TCD mice with the Armstrong strain of LCMV, which causes an acute infection that is cleared within a week by CD8^{+} T cells in WT mice independently of CD4^{+} T cells. In UTX-TCD mice, the loss of UTX had a minimal effect on virus clearance; 6 of 7 UTX-TCD mice resolved the infection by day 8 and only one mouse showed a low level of virus at this time (Figure S2A). Tetramer staining revealed that the total numbers of LCMV-specific Db/GP33-41^{+} CD8^{+} and I-Ab/GP66-77^{+} CD4^{+} T cells 8 days after infection were unaffected by the absence of UTX (Figure S2B). Furthermore, the total numbers of cytokine producing CD8^{+} and CD4^{+} T cells 8 days post infection (pi) were unchanged in the UTX-TCD mice (Figures S2C & S2D). These data show that virus-specific UTX-deficient T cells accumulate and function normally following acute infection. Furthermore, the numbers of cytokine-producing memory T cells at day 66 pi were not altered in the UTX-TCD mice (Figures S2E & S2F). Thus, despite reductions in peripheral T cell numbers under homeostatic conditions (Fig S1B-C), these reductions can be overcome since UTX-TCD mice generate protective antiviral responses following an acute viral infection.

T cell UTX is required for clearance of chronic viral infection

In contrast to the Armstrong strain, the A22 strain of LCMV establishes a chronic infection that typically persists for 1-2 months in WT mice (van der Most et al., 1996; Whitmire et al., 2009). Whereas clearance of the Armstrong strain of LCMV is solely dependent on CD8^{+} T cells, the eventual clearance of persistent LCMV strains, including A22, depends on CD8^{+} T cells, CD4^{+} T cells, and B cells (Bergthaler et al., 2009; Matloubian et al., 1994; Planz et al., 1997). Given the different immune effector requirements for clearing chronic infection, we

tested the effects of T cell specific UTX deficiency on the control of persistent LCMV-A22 infection. There was a delay in the clearance of LCMV-A22 from the serum of the UTX-TCD mice (Figure 1A). The initial levels of virus in the serum were equivalent in the two groups, but the WT animals subsequently eliminated the infection while the UTX-TCD mice did not (Figure 1A). The virus levels in the liver, lung, and kidney were all higher at day 66 pi in the UTX-TCD mice compared to WT mice (Figure 1B).

Because $CD4^+$ and $CD8^+$ T cells are required to eliminate chronic LCMV infection, we examined whether UTX deficiency affects virus-specific $CD4^+$ and/or $CD8^+$ T cell responses. Given that antiviral T cells are affected by viral loads during the chronic stage (Fahey et al., 2011; Fuller and Zajac, 2003; Mueller and Ahmed, 2009; Zajac et al., 1998), we analyzed T cell responses at day 21 pi, when virus levels were equivalent between the WT and UTX-TCD mice. At this time point, any alterations in the T cell responses should be independent of the secondary effects caused by variations in virus load. We did not detect any difference in the frequency or number of tetramer positive UTX-TCD $CD8^+$ T cells at this time point compared to infected WT mice (Figure 1C). Furthermore, there was no difference in $CD8^+$ T cell expression of the “exhaustion” markers, PD-1 and Lag-3 (lymphocyte activation gene-3 or CD223) (Figure 1D). Although $CD8^+$ T cell responses were largely unchanged, UTX-TCD mice demonstrated a reduced frequency and number of LCMV-specific antiviral $CD4^+$ T cells at day 21 (Figure 1E). These data indicate that T cell expression of UTX is critical for the clearance of a chronic virus infection and raise the possibility that UTX directly regulates $CD4^+$ T cell responses.

$CD4^+$ Tfh cell numbers and function are decreased in UTX-TCD mice

$CD4^+$ T cells and antibody production by B cells are crucial for resolving chronic viral infections (Bergthaler et al., 2009; Planz et al., 1997; Richter and Oxenius, 2013). There is an increase in $CD8^+$ T cell exhaustion and delayed virus clearance when $CD4^+$ T cells are depleted during chronic LCMV infection (Matloubian et al., 1994). During these chronic infections, $CD4^+$ T cells preferentially differentiate into Tfh cells, which upregulate CXCR5, migrate into B cell follicles, interact with B cells at germinal centers (GC), and promote the production of antibodies (Crotty, 2011). During these T-B interactions within the GCs, B cells proliferate, mutate their antibody genes, and undergo immunoglobulin class switching; these events are important in the production of protective antibody responses. Based on this and the observed overall reduction in $CD4^+$ T cells, we hypothesized that T cell UTX deficiency may affect $CD4^+$ Tfh cell numbers and/or function.

We measured Tfh cell generation in WT and UTX-TCD mice at day 21 pi to determine the effect of UTX on Tfh differentiation during chronic virus infection. Notably, a population of $CD4^+$ T cells in WT animals co-expressed the Tfh markers CXCR5 and PD-1 (programmed cell death protein 1), while the frequency and total numbers of this population were significantly reduced in UTX-TCD mice (Figure 2A). The reduced cellularity was specific to the Tfh pathway, as the number of Tbet $(TBX21)^+$ Th1 cells was not impacted by loss of UTX (Figure 2B). In addition to the decreased number of Tfh cells, $CXCR5^+$ cells from UTX-TCD mice showed significant reduction in the expression of multiple Tfh-related cell surface molecules involved in cellular interactions with B cells, including ICOS, which

instructs Tfh development through upregulation of BCL-6 (Choi et al., 2011); SLAMF6 (Ly108), a receptor that sustains signals into Tfh cells via SAP (Sh2d1a), and stimulates GC formation (Kageyama et al., 2012); as well as PD-1, OX-40 (CD134 or Tnfrsf4), CD84, and CD200 (Figures 2C and S3A-D). During chronic virus infection, Tfh cells co-express IFNγ and IL-21 (Elsaesser et al., 2009), and we found that the number of $IFN\gamma^{+}IL\text{-}21^{+}$ Tfh cells was decreased in UTX-TCD mice (Figure 2D). The total number of $CXCR5^{+}$ $BCL\text{-}6^{+}$ Tfh cells was also reduced, without affecting the intensity of BCL-6 staining (Figure S3E,F). Thus, UTX-TCD Tfh cells are reduced in number and show decreased expression of Tfh-related effector molecules during chronic infection.

Since Tfh cells function to induce B cell antibody production in the GCs of lymphoid organs, we next determined the effects of T cell UTX deficiency on B cell responses. At day 21 pi, we detected significant decreases in the frequency and total numbers of $Fas^{+}GL7^{+}$ GC B cells by flow cytometry (Figure 2E). Moreover, immunohistochemical staining for peanut agglutinin $(PNA)^{+}$ GC B cells showed significantly decreased areas of GC B cells relative to $B220^{+}$ follicles in UTX-TCD spleens (Figure 2F). Consistent with the reduction in GC B cells, the levels of anti-LCMV total-IgG, IgG1, and IgG2c were decreased in UTX-TCD mice at day 21 pi (Figure 2G & S3G). These findings suggest that T cell expression of UTX maintains Tfh cell differentiation and subsequent B cell antibody production.

UTX intrinsically affects Tfh cell numbers during late chronic virus infection

Although the data above implicate UTX in Tfh development and subsequent antibody production during chronic virus infection, a potential concern is that all T cells in the UTX-TCD mice lack UTX, including $CD8^{+}$ T cells, $CD4^{+}$ T cells, and regulatory $CD4^{+}$ T cell populations. Thus, the effects that we observe for Tfh cells could be an indirect result of the immunological environment within the UTX-TCD mice. Alternatively, UTX could have a cell-intrinsic role in the differentiation of $CD4^{+}$ T cells into the Tfh lineage. To distinguish between these two possibilities, we performed adoptive transfers of virus-specific WT or UTX-TCD naïve $CD4^{+}$ T cells into wildtype hosts and compared the differentiation of the donor cell populations. UTX-TCD mice were crossed with LCMV-specific TCR transgenic SMARTA mice (Oxenius et al., 1998) that express the congenic Ly5a (CD45.1) allele to generate UTX-TCD SMARTA mice. Splenocytes from WT SMARTA mice or UTX-TCD SMARTA mice were adoptively transferred to wildtype $Ly5b^{+}$ (CD45.2) C57BL/6 mice, and recipients were infected with the acute Armstrong strain (Figures S4A) or chronic A22 strain. The WT and UTX-TCD SMARTA cells were detected in equivalent proportions in uninfected control mice, indicating that their engraftment and maintenance was similar in the absence of infection (Figure S4B, left). In response to acute Armstrong infection there was no difference in expansion of SMARTA $CD4^{+}$ T cells or their co-expression of CXCR5 and PD-1 by day 8-9 (Figure S4B-D). In response to chronic A22 virus infection, the WT and UTX-TCD SMARTA cells expanded similarly (d8-9) and were maintained equivalently at d22-23 (Figure 3A), indicating that T cell accumulation and survival are not grossly modulated by UTX. However, by day 22 pi there was a decrease in the frequency and total number of $CXCR5^{+}PD\text{-}1^{+}$ UTX-TCD SMARTA Tfh cells (Figures 3B-D). In addition to their reduced abundance, the UTX-deficient Tfh cells expressed lower amounts of the Tfh effector molecule SLAMF6 at days 8 and 22 pi, and lower ICOS at day 22 pi (Figure 3E).

Whether changes in UTX transcript levels over time may modulate Tfh differentiation was tested in WT SMARTA cells. UTX mRNA was stable across time during the chronic infection and also found at similar levels at day 8 of the acute infection (Figure 3F), indicating that differences in UTX mRNA do not correlate with Tfh differentiation in these cells. In contrast, BCL-6 expression levels directly correlated with the frequency of Tfh cells among the WT SMARTA cells (Figure 3G). Taken together, these data show that UTX has a cell-intrinsic function in $CD4^+$ T cells that is crucial for Tfh cell accumulation during an ongoing chronic virus infection.

Despite similar WT and UTX-TCD SMARTA Tfh cell numbers at day 8 of the acute and chronic infections (Figures 3D & S4D), we observed reduced expression of the Tfh effector molecule SLAMF6 in the absence of UTX (Figure 3E), suggesting that Tfh function may be altered early during infections. To test this, we analyzed endogenous Tfh differentiation and function at day 8 in WT and UTX-TCD mice. We found that Tfh cell numbers were equivalent at day 8 of acute and chronic infections (Figure S5A), which was consistent with the SMARTA findings (Figure 3D). We also observed reduced expression of SLAMF6 on the $CXCR5^+$ cells from the UTX-TCD mice (Figure S5B). T cell UTX deficiency resulted in reduced B cell responses, as measured by serum anti-LCMV total IgG, and germinal center and plasmablast B cell numbers, during acute and chronic infections (Figures S5C,D). These data suggest that even when found at similar quantities, the UTX-deficient Tfh cells are qualitatively affected. Importantly, this functional impairment at early and late stages of chronic infection is not due to enhanced total Treg or T follicular regulatory cell (Tfr) subsets (Figure S5E).

UTX deficiency alters Tfh gene expression via H3K27me3 regulation

To understand how UTX alters global gene expression during Tfh cell specification, we performed RNA-seq expression analysis of endogenous, polyclonal $CD4^+CXCR5^+CD62Llo$ Tfh cells that were FACS-sorted from day 21 A22-infected WT and UTX-TCD mice. In UTX-TCD compared to WT Tfh cells, we identified 54 genes with significantly reduced expression and 34 with increased expression (Figure 4A & Table S1). Among the differentially expressed genes in the UTX-TCD Tfh cells, several Tfh-related genes were down-regulated while T helper type 1 (Th1)-related genes were up-regulated (Figure 4B). Expression of Tfh-related genes such as *Icos*, *Ox-40*, *Il6ra*, and *Slamf6* were all significantly reduced in UTX-TCD Tfh cells. The decreased mRNA for these genes is consistent with decreased protein levels (Figures 2C & S3). In contrast, Th1-associated genes such as *Eomes*, *Ccl4*, *Ccl5*, and *Ccr2* were significantly enhanced in UTX-TCD Tfh cells (Figure 4B). Th1 enhancement has been reported to occur concurrently with loss of Tfh signaling during viral infection (Ray et al., 2014). These findings suggest that UTX enforces a pattern of Tfh gene expression with repression of Th1 genes. Additionally, other genes, such as *Ahnak*, *Tnfrsf25*, and *Thy1*, that are associated with T cell homeostasis, activation, or proliferation were also affected by the absence of UTX (Haeryfar and Hoskin, 2004; Matza and Flavell, 2009; Schreiber and Podack, 2013).

Prevalent UTX-dependent gene activation occurs via H3K27me3 demethylation. To determine if the altered gene expression in UTX-TCD cells is due to the loss of UTX-

mediated histone demethylation, H3K27me3 ChIP-seq was performed on endogenous, polyclonal Tfh cells ($CD4^+CXCR5^+CD62Llo$) sorted at day 21 pi. EdgeR statistical analysis identified all promoter regions (transcription start site +/− 1KB) that experienced significantly elevated H3K27me3 in UTX-TCD cells. To facilitate a broad genomic comparison of UTX affected genes, we measured H3K27me3 accumulation at the promoters of all genes that experienced significantly down-regulated expression in UTX-TCD Tfh (Table S1). A subset of genes with reduced expression also demonstrated significant accumulation of promoter H3K27me3 (6 of 54 genes: *Cd9*, *Evl*, *Il6ra*, *S1pr1*, *Tnfrsf25, and Thy1*). The UCSC genome browser H3K27me3 ChIP-seq tracks for these genes are depicted in Figure 5A. All of the genes identified in Figure 5A by ChIP-Seq showed increased amounts of H3K27 in UTX-TCD cells when analyzed by ChIP-qPCR (Figure 5B). In contrast, several genes with promoters containing H3K27me3 (*Gata3*, *Hoxb1*, *Eomes*) in WT Tfh cells did not show increases in H3K27me3 accumulation in UTX-TCD Tfh cells (Figure 5B and data not shown). The boxplot of log fold change (FC) for H3K27me3 demonstrates that the overall distribution of genes that were down-regulated in UTX-TCD, as revealed by RNA-seq, is significantly increased in H3K27me3 relative to the genes that were up-regulated in UTX-TCD cells (p-value=0.021, Figure 5C). H3K27me3 ChIP-qPCR confirmed that there was an enriched distribution of H3K27me3 in UTX-TCD down-regulated genes (p-value=0.008, Figure 5D). Furthermore, UTX ChIP-qPCR demonstrated enriched UTX occupancy at the promoters of two targets of UTX H3K27 demethylation (*Il6ra* and *Thy1*; Figure S6A). Therefore, the genes with elevated H3K27me3 levels in UTX-TCD Tfh are likely to be gene-specific UTX dependent targets.

During murine chronic virus infection with LCMV-Clone13, irradiation resistant cells produce IL-6 in a biphasic manner, with the second IL-6 peak playing a critical role in virus control (Harker et al., 2011). Consistent with that report, LCMV-A22 infection induced biphasic IL-6 production with a second peak around day 20 during infection. (Figure S6B). The second IL-6 peak acts upon IL-6R on $CD4^+$ T cells to drive Tfh differentiation (Harker et al., 2011; Petrovas et al., 2012). Due to its function in Tfh differentiation during the late phase of chronic viral infection, *Il6ra* stood out among genes identified with H3K27me3 promoter accumulation at day 21 p.i. with LCMV-A22. ChIP-qPCR validated a 3.6 fold accumulation of H3K27me3 at the *Il6ra* promoter in UTX-TCD Tfh relative to WT at day 21 p.i. (Figure 5B). The dynamics of *Il6ra* demethylation and expression were assessed across a time-course using cells from uninfected mice (naïve; $CD62L^{hi}$) and from day 8 (CD62Llo) and day 21 ($CXCR5^+CD62Llo$) after LCMV-A22 infection. *Il6ra* was devoid of H3K27me3, and high levels of IL6Rα protein were expressed on naïve cells from both WT and UTX-TCD mice (Figure 5E-G). Early in LCMV-A22 infection (d8), *Il6ra* accumulated H3K27me3 and there were reduced amounts of IL6Rα protein in both WT and UTX-TCD cells. However in the later phase of chronic infection (d21), WT Tfh cells had elevated IL6Rα expression while UTX-TCD Tfh cells had enhanced *Il6ra* H3K27me3 accumulation and reduced IL6Rα protein. To determine the functional significance of the reduced IL-6 receptor expression on UTX-TCD cells, we compared the responsiveness of UTX-TCD and WT T cells to IL-6 *in vitro*. IL-6-induced phosphorylation of STAT3 was unchanged between WT and UTX-TCD naïve $CD4^+$ T cells from uninfected mice and effector cells from day 8 LCMV-A22 infected mice (Figure S6C-D). However at day 21, the

phosphorylation of STAT3 was reduced in UTX-TCD compared to WT T cells following *in vitro* culture with IL-6 (Figure 5H). In contrast, IL-21 stimulated equivalent phospho-STAT3 levels in WT and UTX-TCD cells, indicating that the defect seen in response to IL-6 is not due to an inherent defect in STAT3 (Figure 5H). These results suggest that UTX-mediated H3K27me3 demethylation is a dynamic process that occurs during the course of a chronic virus infection to enforce appropriate IL-6Rα expression and downstream function, which includes the promotion of Tfh differentiation.

UTX expression is gene-dosage dependent and decreased in Turner Syndrome

Utx escapes X-inactivation in both humans and mice (Greenfield et al., 1998). Thus, UTX is expressed by both X chromosomes in females. Whether UTX function in T cells is dosage dependent, however, is not known. We investigated the effects of UTX dosage on the control of chronic virus infection in mice heterozygous for *Utx* mutation (*Utx*$^{+/fl}$*Lck-Cre;* UTX-THet). Cohorts of UTX-WT, UTX-THet, and UTX-TCD were given LCMV-A22, and viral loads and T cell responses were followed over time. The clearance of LCMV-A22 from the serum was delayed in UTX-THet mice compared to WT mice, but the phenotype was not as severe as in UTX-TCD mice (Figure 6A). Likewise, the UTX-THet mice showed intermediate titres of infectious virus in several tissues at day 55 pi (Figure 6B). The UTX-TCD mice show reduced Tfh differentiation (Figures 2-3), which likely contributed to the delay in resolving LCMV-A22. Similarly, the UTX-THet mice had fewer Tfh cells at day 20 (Figures 6C & 6D). These data indicate that a 50% reduction in UTX expression diminishes the formation or maintenance of Tfh cells and impairs immune protection against a chronic virus infection.

UTX gene-dosage dependency is potentially of clinical relevance in humans. Turner Syndrome (TS) occurs in females lacking part or all of an X chromosome and is the most common sex chromosomal abnormality that affects girls and women. TS is characterized by an array of clinical conditions, including recurrent ear infections and alterations in T cell and immunoglobulin subsets, though the mechanisms underlying these immune changes are not currently known (Cacciari et al., 1981; Jensen et al., 1976; Mock et al., 2000; Stenberg et al., 1998; Su et al., 2009). Because TS subjects lack at least part of the second sex chromosome, decreased expression of X-linked gene(s) that escape X-inactivation may underlie these immune alterations (Carrel and Willard, 2005). Importantly, *UTX* is located on the X chromosome and escapes X-inactivation in both mice and humans (Greenfield et al., 1998). Given that *UTX* is subject to gene dosage effects, we reasoned that *UTX* might be haploinsufficient in TS immune cells.

We utilized global gene expression profiling using the Agilent SurePrint G3 Human Gene Expression 8×60K Microarray to identify candidate genes with altered expression in TS immune cells. Comparison of peripheral blood mononuclear cells (PBMCs) from control females to TS subjects with confirmed 45X karyotype showed differential expression of 1169 unique genes, including 35 that are located on the X chromosome. *UTX* was among the 10 genes with the largest decrease in expression in TS subjects (Figure 7A) and the only gene among these candidates known to escape X-inactivation (Greenfield et al., 1998). The decrease in *UTX* transcript expression was verified by RT-PCR on cDNA from TS and

female control PBMCs (Figure 7B). These findings suggest a potential causative role for UTX deficiency in TS immune dysfunction.

We sought to determine if decreased UTX expression in TS might be associated with decreases in Tfh cells, as we have observed in mice. As expected, the majority of TS individuals had a history of recurrent otitis media (Figure S7A). We first measured the frequency of total, naïve ($CD45RA^+$) and antigen experienced ($CD45RO^+$) $CD4^+$ T cells, and found no significant differences between controls and TS individuals (Figure 7C-E). Circulating $CD4^+CXCR5^+$ have been correlated with antibody production in humans, thus representing an accessible, surrogate Tfh-like population (Morita et al., 2011; Pallikkuth et al., 2012; Simpson et al., 2010). We therefore compared the frequency of circulating $CD4^+$ $CXCR5^+$ T cells in non-TS females versus TS subjects. There was a two-fold reduction in the frequency of circulating $CD4^+CXCR5^+$ cells from TS subjects (Figure 7F,G). The expression of IL-6R on $CXCR5^+$ $CD4^+$ T cells was modestly decreased in TS subjects, although this difference did not reach statistical significance because of an outlier in the control group (Figure S7B). Additionally, the $CXCR5^+$ cells from TS subjects showed a trend towards diminished responsiveness to IL-6-induced phosphorylation of STAT3 compared to cells from controls (Figure S7C). Together, these findings suggest that UTX deficiency may contribute to the infection predisposition observed in TS by reducing the frequency of the $CD4^+$ $CXCR5^+$ subset.

Discussion

T cell subset differentiation is highly regulated to ensure that the adaptive immune system can vigorously fight off diverse pathogens while avoiding immune-mediated pathology. Th subtypes are characterized by distinct H3K27me3 epigenetic profiles that reflect subtype specific transcriptional programs (Wei et al., 2009). These lineage specific epigenetic changes suggest that histone-modifying enzymes are crucial in their differentiation. In this study, we identify the H3K27me3 demethylase UTX as a key regulator of $CD4^+$ T cell differentiation to the Tfh subset during a chronic virus infection. In the absence of UTX we observe decreased numbers of Tfh cells, altered germinal centers, reduced humoral immune responses and enhanced virus persistence.

Tfh cells are crucial in vaccine responses and protection from infection via their ability to promote B cell antibody production and affinity maturation. Recent data in mice and humans have demonstrated that chronic virus infections result in enhanced Tfh differentiation (Fahey et al., 2011; Feng et al., 2012; Feng et al., 2011; Lindqvist et al., 2012). Interestingly, the development of Tfh cells appears to be differentially regulated in response to acute versus chronic virus infections. IL-6 and its cognate receptor (IL-6Rα) are required for Tfh differentiation during chronic LCMV infection of mice and are strongly correlated with Tfh responses following SIV infection of macaques (Harker et al., 2011; Petrovas et al., 2012). Our data indicate that UTX-TCD Tfh cell frequency was unchanged during acute infection and early during chronic infection (Figures 3, S4, & S5). However, the accumulation of UTX-TCD Tfh cells was reduced later during the chronic infection. Additionally, our data indicate that the responsiveness of $CD4^+$ T cells towards IL-6 is regulated by UTX-mediated H3K27me3 demethylation of the *Il6ra* promoter during later

stages of chronic infection. Together, these findings suggest that epigenetic regulation of *Il6ra* by UTX may underlie the differences seen in acute versus chronic infection.

In addition to the effects of UTX on the number of Tfh cells at later times during chronic virus infection, UTX also appears to regulate the function of Tfh cells throughout acute and chronic infection. At day 8 pi the number of Tfh cells was equivalent, yet the B cell response was decreased in UTX-TCD in comparison with WT mice. One possibility is that T cell recruitment into B cell follicles is defective in the absence of UTX. Another possibility is that T-B interactions, which are dependent upon the adaptor protein SAP, are disrupted in the absence of T cell UTX. We noted a consistent reduction in expression of SLAMF6, which promotes T-B interactions and recruits SAP, across all time points in UTX deficient T cells. Therefore, UTX mediated regulation of SLAMF6 may be involved in promoting Tfh cell functionality. Further experiments are needed to determine at what step T cell help for B cells is defective, as well as to test if SLAMF6 or other specific targets of UTX regulate this pathway.

Interestingly, IL-6 expression during chronic LCMV infection is biphasic, with an early induction followed by silencing and then a second wave of expression a few weeks later (Harker et al., 2011). Given that UTX-TCD Tfh cell frequency was unchanged during the early stage of chronic infection (Figure 3 and S5), we propose that early robust inflammatory signals, potentially including IL-6, are sufficient to induce Tfh cell development in the absence of UTX, as T cell expression of IL-6Rα is UTX-independent in naïve cells and at day 8 (Figure 5). However, in the context of sustained infection, UTX-mediated demethylase activity is required to ensure that virus-specific Tfh cells are receptive to the second wave of IL-6 expression. Compared to antibody responses to acute infections or vaccines, neutralizing antibody to chronic virus infections often emerge following a lengthy delay and are thought to require extensive somatic hypermutation of immunoglobulin in GCs. Thus, it is plausible that T cell UTX plays a central role in the formation of neutralizing antibody during this delayed phase.

Global transcriptome analysis identified multiple genes with reduced expression in UTX-TCD cells, and a small number of those genes (e.g., *Il6ra*) had enhanced H3K27me3, indicating that UTX demethylase activity contributes to their expression. It was surprising that such a small number of genes showed enhanced H3K27me3 and reduced expression in the absence of UTX. One explanation for this may be a potential overlap in targets between UTX and JMJD3, the other H3K27me3 demethylase expressed in T cells. In addition to the genes dependent on UTX-mediated demethylation, the expression of several other Tfh lineage genes in UTX-TCD cells were reduced in the absence of H3K27me3 accumulation (e.g., *Slamf6*, Figure 5B). There are two possible explanations for these UTX-dependent changes in gene expression. It could be that these genes are not direct targets of UTX regulation but are induced by factors, such as activated STAT3, that are downstream of IL-6 signaling that is potentiated by UTX. Alternatively, it could be that these genes are induced by UTX in a demethylase-independent manner, which has been observed in a number of developmental settings. For example, UTX, as well as JMJD3, was able to drive IFN-γ and other cytokine production in an EL4 lymphoma line through interactions with T-box transcription factors and nucleosome remodeling factors (Miller et al., 2010). UTX may act

in a similar fashion during Tfh differentiation by interacting with and promoting the activity of Tfh-specific transcription factors independently of its H3K27me3 demethylase ability.

Finally, our study of TS subjects suggests a potential role for UTX in human T cells. Recurrent ear infections in TS are well-recognized, but the underlying mechanism for this is not known (Stenberg et al., 1998). A study seeking to associate recurrent ear infections in TS with immune abnormalities did not find major immunological deficiencies in TS patients (Stenberg et al., 2004). However, other investigations have demonstrated abnormalities in the T cell compartment and the generation of immunoglobulins, suggesting that recurrent ear infections might reflect a defect in immune function (Cacciari et al., 1981; Jensen et al., 1976; Mock et al., 2000). In line with the latter studies, our analysis demonstrates that TS immune cells are UTX deficient and the frequency of circulating $CD4^+$ $CXCR5^+$ T cells is reduced in TS. A caveat to this result, however, is that circulating $CD4^+$ $CXCR5^+$ T cells likely represent a heterogeneous population (He et al., 2013; Locci et al., 2013). Interestingly, UTX mutations have recently been described in Kabuki Syndrome, a rare congenital disorder in which susceptibility to infections has also been described (Lederer et al., 2012). Remarkably, recurrent ear infections also occur in 63% of Kabuki Syndrome patients (Matsumoto and Niikawa, 2003). Thus, two independent syndromes associated with a loss of UTX function share increased susceptibility to chronic ear infection. Our findings describing the role of UTX in $CD4^+$ T cells provide a mechanism for the immune dysfunctions in these two syndromes.

Experimental Procedures

See Supplemental Experimental Procedures for details.

Mice

All mouse experimental procedures were approved by the University of North Carolina Institutional Animal Care and Use Committee. $Utx^{fl/fl}$ mice were backcrossed to C57BL/6J for > 5 generations. These mice were then crossed to *Lck-Cre* (Hennet et al., 1995) and $Ly5a^+$ (CD45.1) SMARTA TCR-transgenic lines that have $CD4^+$ T cells specific for the LCMV epitope $GP_{61\text{-}80}$ presented by $I\text{-}A^b$ (Oxenius et al., 1998). All mouse experimental procedures were approved by the University of North Carolina Institutional Animal Care and Use Committee.

Virus

Mice were infected by intraperitoneal injection of 2×10^5 PFU of LCMV-Armstrong or intravenous injection of 2×10^6 PFU LCMV-A22. LCMV was prepared from BHK cells and quantified by plaque assay on Vero cell monolayers.

RNA-seq

RNA was extracted from FACS-sorted $CD4^+CXCR5^+CD62L^{lo}$ T cells (10^6 cells total) from day 21 pi and purified on oligo(dT) dynabeads for cDNA amplification. Adaptors were ligated and 100bp reads were sequenced by the HiSeq 2000 Analyzer located at the Scripps DNA Sequencing Facility.

Human samples

All human research was approved by the University of North Carolina Institutional Review Board, and written informed consent was obtained from all participants. PBMC RNA from ten Turner Syndrome subjects and five control female subjects were labeled and hybridized to the Agilent SurePrint G3 Human Gene Expression 8×60K Microarray. In the case where microarray chips were scanned on different dates, batch effect was identified and removed (Partek® Genomics Suite™, St. Louis, MO). See Supplemental Experimental Procedures for analysis details.

Adoptive Transfers

Spleen cells were isolated from WT or UTX-TKO Ly5a^{+} SMARTA TCR transgenic mice. The frequency of CD4^{+} T cells was determined by flow cytometry, and the spleen cells were adjusted so that 5×10^{3} Smarta CD4^{+} T cells were injected into WT C57BL/6 mice (Ly5b^{+}Ly5a^{-}) via tail vein injection. The cells were allowed to engraft for 4 days before the recipient mice were infected.

Antibody levels

Sera were collected and virus-specific IgG was measured by ELISA using plates coated with virus-infected or uninfected BHK lysates (Whitmire et al., 1996). The highest dilution at which the OD value reached 1.5 (roughly 50% maximal response) was calculated for each sample.

Immunohistochemistry

Formalin-fixed paraffin-embedded spleen sections were stained with fluorescent antibodies or peanut-agglutinin and imaged on a Zeiss-710 confocal laser scanning microscope at the UNC Microscopy Services Laboratory.

Phospho-STAT3 staining

Mouse splenocytes or human PBMCs were cultured with recombinant mouse or human IL-6, respectively (both from Peprotech). The cells were then surface stained, fixed, permeabilized with Perm Buffer III (BD Biosciences) and stained with mouse anti-human STAT3 (pS727) Clone 49/p-STAT3 (BD Biosciences).

ChIP

FACS-sorted CD4^{+}CXCR5^{+}CD62L^{lo} T cells (2×10^{6} cells per replicate) from day 21 pi were crosslinked with 0.6% formaldehyde and sonicated (Bioruptor Sonifier). ChIP was performed with anti-H3K27me3 (Abcam ab6002, 2μg) (Rahl et al., 2010). UTX ChIP was performed on in vitro differentiated Tfh (Lu et al., 2011) and 1×10^{7} nuclei were subjected to micrococcal nuclease digestion (2,000U/ml for 15 minutes at 37 degrees) prior to ChIP with UTX antibody (Agger et al., 2007).

Statistics

All bar graphs are presented as mean + SEM. Significance was determined by unpaired Students *t* test. * P < 0.05, ** P <0.01, and *** P <0.001.

Supplementary Material

Refer to Web version on PubMed Central for supplementary material.

Acknowledgements

Kristian Helin (University of Copenhagen, Denmark) kindly provided the UTX antibody for ChIP analysis. NCTracs (50K Pilot Grant to MAS); NIH (R01 NS079683 to MAS; R01 AI074862 and R56 AI110682 to JKW; T32 AI7273-27 to KDC; and R01 GM10974 to TM, KBS and JS); NC TraCS Translational Team Science Award (TTSA004P2), and start-up funds from UNC-Chapel Hill to MAS and JKW. The UNC Flow Cytometry Core Facility is supported in part by P30 CA016086 Cancer Center Core Support Grant to the UNC Lineberger Comprehensive Cancer Center.

References

Agger K, Cloos PA, Christensen J, Pasini D, Rose S, Rappsilber J, Issaeva I, Canaani E, Salcini AE, Helin K. UTX and JMJD3 are histone H3K27 demethylases involved in HOX gene regulation and development. Nature. 2007; 449:731–734. [PubMed: 17713478]

Bannister AJ, Kouzarides T. Regulation of chromatin by histone modifications. Cell Res. 2011; 21:381–395. [PubMed: 21321607]

Bergthaler A, Flatz L, Verschoor A, Hegazy AN, Holdener M, Fink K, Eschli B, Merkler D, Sommerstein R, Horvath E, et al. Impaired antibody response causes persistence of prototypic T cell-contained virus. PLoS biology. 2009; 7:e1000080. [PubMed: 19355789]

Brooks DG, Teyton L, Oldstone MB, McGavern DB. Intrinsic functional dysregulation of CD4 T cells occurs rapidly following persistent viral infection. J Virol. 2005; 79:10514–10527. [PubMed: 16051844]

Cacciari E, Masi M, Fantini MP, Licastro F, Cicognani A, Pirazzoli P, Villa MP, Specchia F, Forabosco A, Franceschi C, Martoni L. Serum immunoglobulins and lymphocyte subpopulations derangement in Turner's syndrome. J Immunogenet. 1981; 8:337–344. [PubMed: 7299139]

Carrel L, Willard HF. X-inactivation profile reveals extensive variability in X-linked gene expression in females. Nature. 2005; 434:400–404. [PubMed: 15772666]

Choi YS, Kageyama R, Eto D, Escobar TC, Johnston RJ, Monticelli L, Lao C, Crotty S. ICOS receptor instructs T follicular helper cell versus effector cell differentiation via induction of the transcriptional repressor Bcl6. Immunity. 2011; 34:932–946. [PubMed: 21636296]

Elsaesser H, Sauer K, Brooks DG. IL-21 is required to control chronic viral infection. Science. 2009; 324:1569–1572. [PubMed: 19423777]

Fahey LM, Wilson EB, Elsaesser H, Fistonich CD, McGavern DB, Brooks DG. Viral persistence redirects CD4 T cell differentiation toward T follicular helper cells. J Exp Med. 2011; 208:987–999. [PubMed: 21536743]

Feng J, Hu X, Guo H, Sun X, Wang J, Xu L, Jiang Z, Xu B, Niu J, Jiang Y. Patients with chronic hepatitis C express a high percentage of CD4(+)CXCR5(+) T follicular helper cells. J Gastroenterol. 2012; 47:1048–1056. [PubMed: 22426636]

Feng J, Lu L, Hua C, Qin L, Zhao P, Wang J, Wang Y, Li W, Shi X, Jiang Y. High frequency of CD4+ CXCR5+ TFH cells in patients with immune-active chronic hepatitis B. PLoS One. 2011; 6:e21698. [PubMed: 21750724]

Frohlich A, Kisielow J, Schmitz I, Freigang S, Shamshiev AT, Weber J, Marsland BJ, Oxenius A, Kopf M. IL-21R on T cells is critical for sustained functionality and control of chronic viral infection. Science. 2009; 324:1576–1580. [PubMed: 19478140]

Fuller MJ, Zajac AJ. Ablation of CD8 and CD4 T cell responses by high viral loads. J Immunol. 2003; 170:477–486. [PubMed: 12496434]

Greenfield A, Carrel L, Pennisi D, Philippe C, Quaderi N, Siggers P, Steiner K, Tam PP, Monaco AP, Willard HF, Koopman P. The UTX gene escapes X inactivation in mice and humans. Hum Mol Genet. 1998; 7:737–742. [PubMed: 9499428]

Haeryfar SM, Hoskin DW. Thy-1: more than a mouse pan-T cell marker. J Immunol. 2004; 173:3581–3588. [PubMed: 15356100]

Harker JA, Lewis GM, Mack L, Zuniga EI. Late interleukin-6 escalates T follicular helper cell responses and controls a chronic viral infection. Science. 2011; 334:825–829. [PubMed: 21960530]

He J, Tsai LM, Leong YA, Hu X, Ma CS, Chevalier N, Sun X, Vandenberg K, Rockman S, Ding Y, et al. Circulating Precursor CCR7(lo)PD-1(hi) CXCR5(+) CD4(+) T Cells Indicate Tfh Cell Activity and Promote Antibody Responses upon Antigen Reexposure. Immunity. 2013; 39:770–781. [PubMed: 24138884]

Hennet T, Hagen FK, Tabak LA, Marth JD. T-cell-specific deletion of a polypeptide N-acetylgalactosaminyl-transferase gene by site-directed recombination. Proc Natl Acad Sci U S A. 1995; 92:12070–12074. [PubMed: 8618846]

Jensen K, Petersen PH, Nielsen EL, Dahl G, Nielsen J. Serum immunoglobulin M, G, and A concentration levels in Turner's syndrome compared with normal women and men. Hum Genet. 1976; 31:329–334. [PubMed: 955627]

Kageyama R, Cannons JL, Zhao F, Yusuf I, Lao C, Locci M, Schwartzberg PL, Crotty S. The receptor Ly108 functions as a SAP adaptor-dependent on-off switch for T cell help to B cells and NKT cell development. Immunity. 2012; 36:986–1002. [PubMed: 22683125]

Lederer D, Grisart B, Digilio MC, Benoit V, Crespin M, Ghariani SC, Maystadt I, Dallapiccola B, Verellen-Dumoulin C. Deletion of KDM6A, a histone demethylase interacting with MLL2, in three patients with Kabuki syndrome. American journal of human genetics. 2012; 90:119–124. [PubMed: 22197486]

Lindqvist M, van Lunzen J, Soghoian DZ, Kuhl BD, Ranasinghe S, Kranias G, Flanders MD, Cutler S, Yudanin N, Muller MI, et al. Expansion of HIV-specific T follicular helper cells in chronic HIV infection. J Clin Invest. 2012; 122:3271–3280. [PubMed: 22922259]

Locci M, Havenar-Daughton C, Landais E, Wu J, Kroenke MA, Arlehamn CL, Su LF, Cubas R, Davis MM, Sette A, et al. Human circulating PD-1+CXCR3-CXCR5+ memory Tfh cells are highly functional and correlate with broadly neutralizing HIV antibody responses. Immunity. 2013; 39:758–769. [PubMed: 24035365]

Lu KT, Kanno Y, Cannons JL, Handon R, Bible P, Elkahloun AG, Anderson SM, Wei L, Sun H, O'Shea JJ, Schwartzberg PL. Functional and epigenetic studies reveal multistep differentiation and plasticity of in vitro-generated and in vivo-derived follicular T helper cells. Immunity. 2011; 35:622–632. [PubMed: 22018472]

Matloubian M, Concepcion RJ, Ahmed R. CD4+ T cells are required to sustain CD8+ cytotoxic T-cell responses during chronic viral infection. J Virol. 1994; 68:8056–8063. [PubMed: 7966595]

Matsumoto N, Niikawa N. Kabuki make-up syndrome: a review. Am J Med Genet C Semin Med Genet. 2003; 117C:57–65. [PubMed: 12561059]

Matza D, Flavell RA. Roles of Ca(v) channels and AHNAK1 in T cells: the beauty and the beast. Immunol Rev. 2009; 231:257–264. [PubMed: 19754902]

Miller SA, Mohn SE, Weinmann AS. Jmjd3 and UTX play a demethylase-independent role in chromatin remodeling to regulate T-box family member-dependent gene expression. Mol. Cell. 2010; 40:594–605. [PubMed: 21095589]

Mock, Markert UR, Vogelsang H, Jager L. Selective T-cell deficiency in Turner's syndrome. J Investig Allergol Clin Immunol. 2000; 10:312–313.

Morita R, Schmitt N, Bentebibel SE, Ranganathan R, Bourdery L, Zurawski G, Foucat E, Dullaers M, Oh S, Sabzghabaei N, et al. Human blood CXCR5(+)CD4(+) T cells are counterparts of T follicular cells and contain specific subsets that differentially support antibody secretion. Immunity. 2011; 34:108–121. [PubMed: 21215658]

Mueller SN, Ahmed R. High antigen levels are the cause of T cell exhaustion during chronic viral infection. Proc Natl Acad Sci U S A. 2009; 106:8623–8628. [PubMed: 19433785]

Oxenius A, Bachmann MF, Zinkernagel RM, Hengartner H. Virus-specific MHC-class II-restricted TCR-transgenic mice: effects on humoral and cellular immune responses after viral infection. Eur J Immunol. 1998; 28:390–400. [PubMed: 9485218]

Pallikkuth S, Parmigiani A, Silva SY, George VK, Fischl M, Pahwa R, Pahwa S. Impaired peripheral blood T-follicular helper cell function in HIV-infected nonresponders to the 2009 H1N1/09 vaccine. Blood. 2012; 120:985–993. [PubMed: 22692510]

Petrovas C, Yamamoto T, Gerner MY, Boswell KL, Wloka K, Smith EC, Ambrozak DR, Sandler NG, Timmer KJ, Sun X, et al. CD4 T follicular helper cell dynamics during SIV infection. J Clin Invest. 2012; 122:3281–3294. [PubMed: 22922258]

Planz O, Ehl S, Furrer E, Horvath E, Brundler MA, Hengartner H, Zinkernagel RM. A critical role for neutralizing-antibody-producing B cells, CD4(+) T cells, and interferons in persistent and acute infections of mice with lymphocytic choriomeningitis virus: implications for adoptive immunotherapy of virus carriers. Proc Natl Acad Sci U S A. 1997; 94:6874–6879. [PubMed: 9192659]

Rahl PB, Lin CY, Seila AC, Flynn RA, McCuine S, Burge CB, Sharp PA, Young RA. c-Myc regulates transcriptional pause release. Cell. 2010; 141:432–445. [PubMed: 20434984]

Ray JP, Marshall HD, Laidlaw BJ, Staron MM, Kaech SM, Craft J. Transcription factor STAT3 and type I interferons are corepressive insulators for differentiation of follicular helper and T helper 1 cells. Immunity. 2014; 40:367–377. [PubMed: 24631156]

Richter K, Oxenius A. Non-neutralizing antibodies protect from chronic LCMV infection independently of activating FcgammaR or complement. Eur J Immunol. 2013; 43:2349–2360. [PubMed: 23749374]

Schreiber TH, Podack ER. Immunobiology of TNFSF15 and TNFRSF25. Immunol Res. 2013; 57:3–11. [PubMed: 24242819]

Shpargel KB, Sengoku T, Yokoyama S, Magnuson T. UTX and UTY demonstrate histone demethylase-independent function in mouse embryonic development. PLoS genetics. 2012; 8:e1002964. [PubMed: 23028370]

Simpson N, Gatenby PA, Wilson A, Malik S, Fulcher DA, Tangye SG, Manku H, Vyse TJ, Roncador G, Huttley GA, et al. Expansion of circulating T cells resembling follicular helper T cells is a fixed phenotype that identifies a subset of severe systemic lupus erythematosus. Arthritis Rheum. 2010; 62:234–244. [PubMed: 20039395]

Stenberg AE, Nylen O, Windh M, Hultcrantz M. Otological problems in children with Turner's syndrome. Hear Res. 1998; 124:85–90. [PubMed: 9822905]

Stenberg AE, Sylven L, Magnusson CG, Hultcrantz M. Immunological parameters in girls with Turner syndrome. J Negat Results Biomed. 2004; 3:6. [PubMed: 15563731]

Su MA, Stenerson M, Liu W, Putnam A, Conte F, Bluestone JA, Anderson MS. The role of X-linked FOXP3 in the autoimmune susceptibility of Turner Syndrome patients. Clin Immunol. 2009; 131:139–144. [PubMed: 19150256]

Thomsen AR, Johansen J, Marker O, Christensen JP. Exhaustion of CTL memory and recrudescence of viremia in lymphocytic choriomeningitis virus-infected MHC class II-deficient mice and B cell-deficient mice. J Immunol. 1996; 157:3074–3080. [PubMed: 8816417]

Tumes DJ, Onodera A, Suzuki A, Shinoda K, Endo Y, Iwamura C, Hosokawa H, Koseki H, Tokoyoda K, Suzuki Y, et al. The polycomb protein Ezh2 regulates differentiation and plasticity of CD4(+) T helper type 1 and type 2 cells. Immunity. 2013; 39:819–832. [PubMed: 24238339]

van der Most RG, Sette A, Oseroff C, Alexander J, Murali-Krishna K, Lau LL, Southwood S, Sidney J, Chesnut RW, Matloubian M, Ahmed R. Analysis of cytotoxic T cell responses to dominant and subdominant epitopes during acute and chronic lymphocytic choriomeningitis virus infection. J Immunol. 1996; 157:5543–5554. [PubMed: 8955205]

Virgin HW, Wherry EJ, Ahmed R. Redefining chronic viral infection. Cell. 2009; 138:30–50. [PubMed: 19596234]

Wei G, Wei L, Zhu J, Zang C, Hu-Li J, Yao Z, Cui K, Kanno Y, Roh TY, Watford WT, et al. Global mapping of H3K4me3 and H3K27me3 reveals specificity and plasticity in lineage fate determination of differentiating CD4+ T cells. Immunity. 2009; 30:155–167. [PubMed: 19144320]

Wherry EJ. T cell exhaustion. Nat Immunol. 2011; 12:492–499. [PubMed: 21739672]

Whitmire JK, Asano MS, Kaech SM, Sarkar S, Hannum LG, Shlomchik MJ, Ahmed R. Requirement of B cells for generating CD4+ T cell memory. J Immunol. 2009; 182:1868–1876. [PubMed: 19201839]

Whitmire JK, Slifka MK, Grewal IS, Flavell RA, Ahmed R. CD40 ligand-deficient mice generate a normal primary cytotoxic T-lymphocyte response but a defective humoral response to a viral infection. J Virol. 1996; 70:8375–8381. [PubMed: 8970958]

Wilson CB, Rowell E, Sekimata M. Epigenetic control of T-helper-cell differentiation. Nat Rev Immunol. 2009; 9:91–105. [PubMed: 19151746]

Yi JS, Du M, Zajac AJ. A vital role for interleukin-21 in the control of a chronic viral infection. Science. 2009; 324:1572–1576. [PubMed: 19443735]

Zajac AJ, Blattman JN, Murali-Krishna K, Sourdive DJ, Suresh M, Altman JD, Ahmed R. Viral immune evasion due to persistence of activated T cells without effector function. J Exp Med. 1998; 188:2205–2213. [PubMed: 9858507]

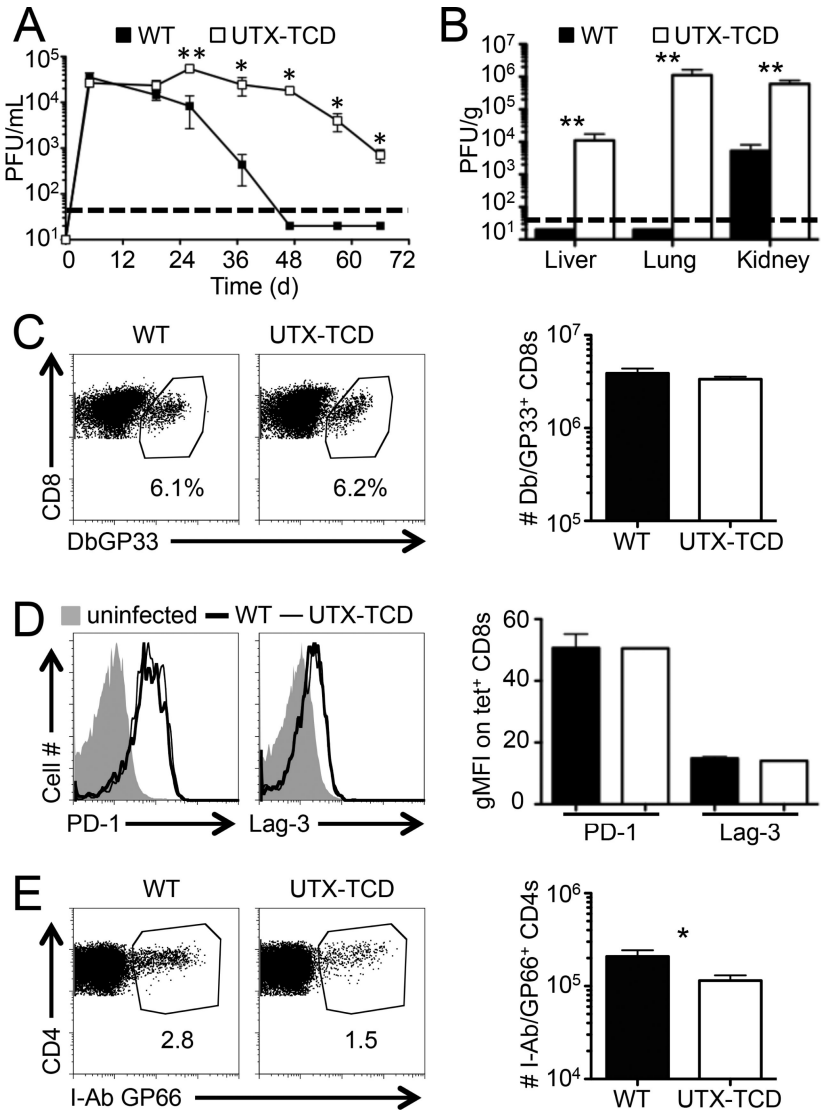

Figure 1. T cell UTX deficiency increases the persistence of a disseminating viral infection

UTX-TCD and UTX-WT littermate control mice were infected with LCMV-A22.

(A) The viral titer in the serum over time.

(B) The level of infectious virus in the indicated tissues at day 66 pi. The dashed lines indicate the level of detection.

(C) Examples of Db/GP33-41 staining of gated $CD8^+CD4^-CD19^-$ T cells (left) and the total number of splenic tetramer positive $CD8^+$ T cells at day 21 pi (right).

(D) Examples of PD-1 and Lag-3 staining (left) and their gMFI on gated tetramer positive $CD8^+$ T cells (right).

(E) Examples of I-Ab/GP66-77 staining of gated $CD4^+CD8^-CD19^-$ T cells (left) and the total number of splenic tetramer positive $CD4^+$ T cells at day 21 pi (right).

All data in this figure are representative of three independent experiments and shown as means ± SEM. See also Figures S1 and S2.

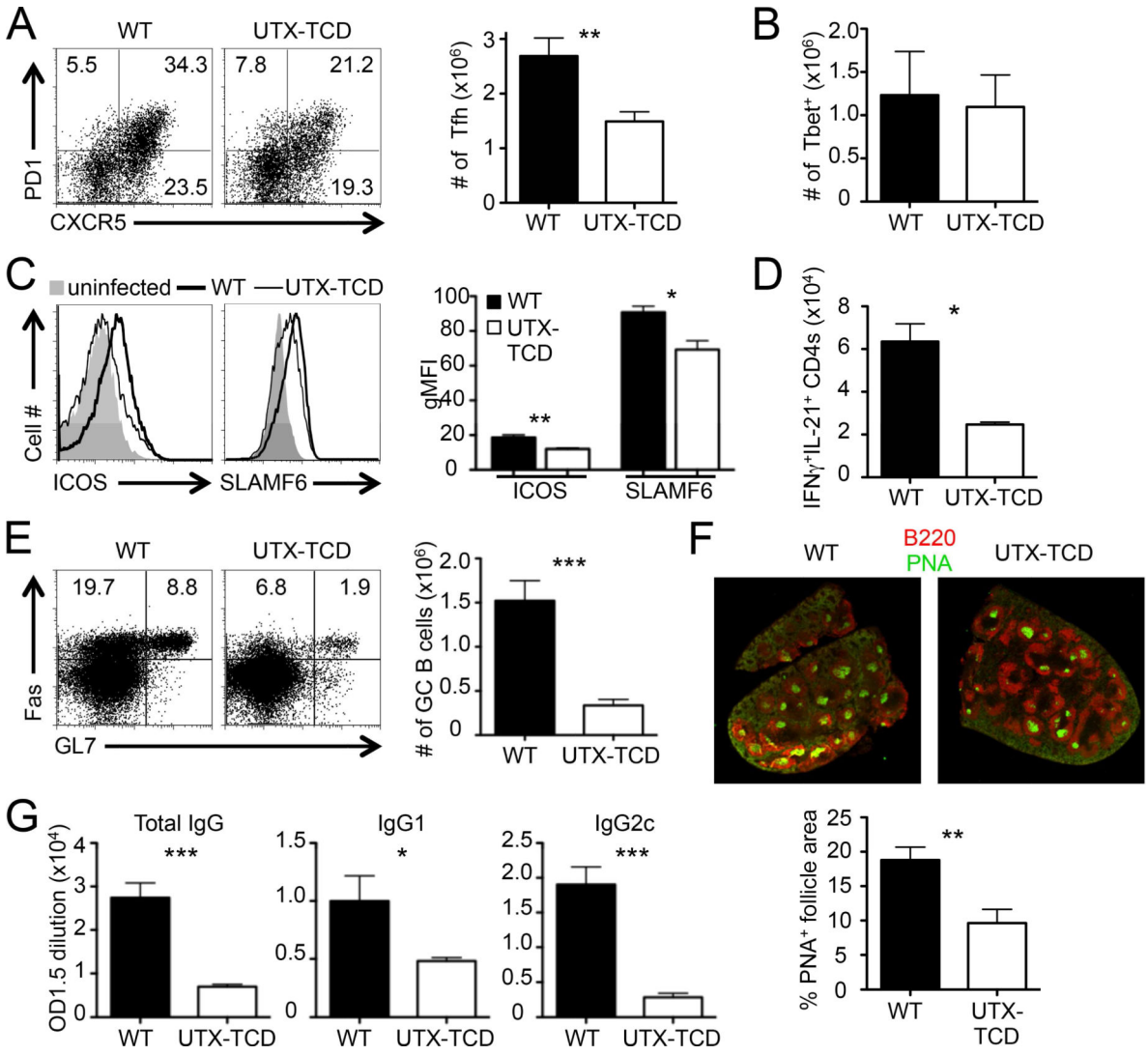

Figure 2. T cell expression of UTX promotes CD4$^+$ Tfh development and B cell function during a chronic viral infection

UTX-TCD and UTX-WT littermate control mice were infected with LCMV-A22 and harvested at d21.

(A) Examples of PD-1 and CXCR5 staining on gated CD4$^+$CD8$^-$CD19$^-$ T cells (left) and the total number of CXCR5$^+$PD-1$^+$ Tfh cells (right).

(B) The total number of T-bet$^+$ CD4$^+$ T cells.

(C) Examples of ICOS and SLAMF6 staining (left) and their gMFI on gated CD4$^+$CXCR5$^+$CD8-CD19$^-$ Tfh cells (right).

(D) The total number of CD4$^+$ T cells producing IFNγ and IL-21, as measured by ICS.

(E) An example of Fas and GL7 staining on gated B220$^+$ cells (left) and the total number of GC B cells (right).

(F) Representative spleen sections stained for B220 and PNA (top), and the percentage of the B220$^+$ area that is also PNA$^+$ (bottom).

(G) The serum concentrations of anti-LCMV total IgG, IgG1, and IgG2c.

Panels A,B,C, E & G are representative of three independent experiments, panel F is of two independent experiments, and panel D is of one experiment; all are shown as means + SEM. See also Figure S3.

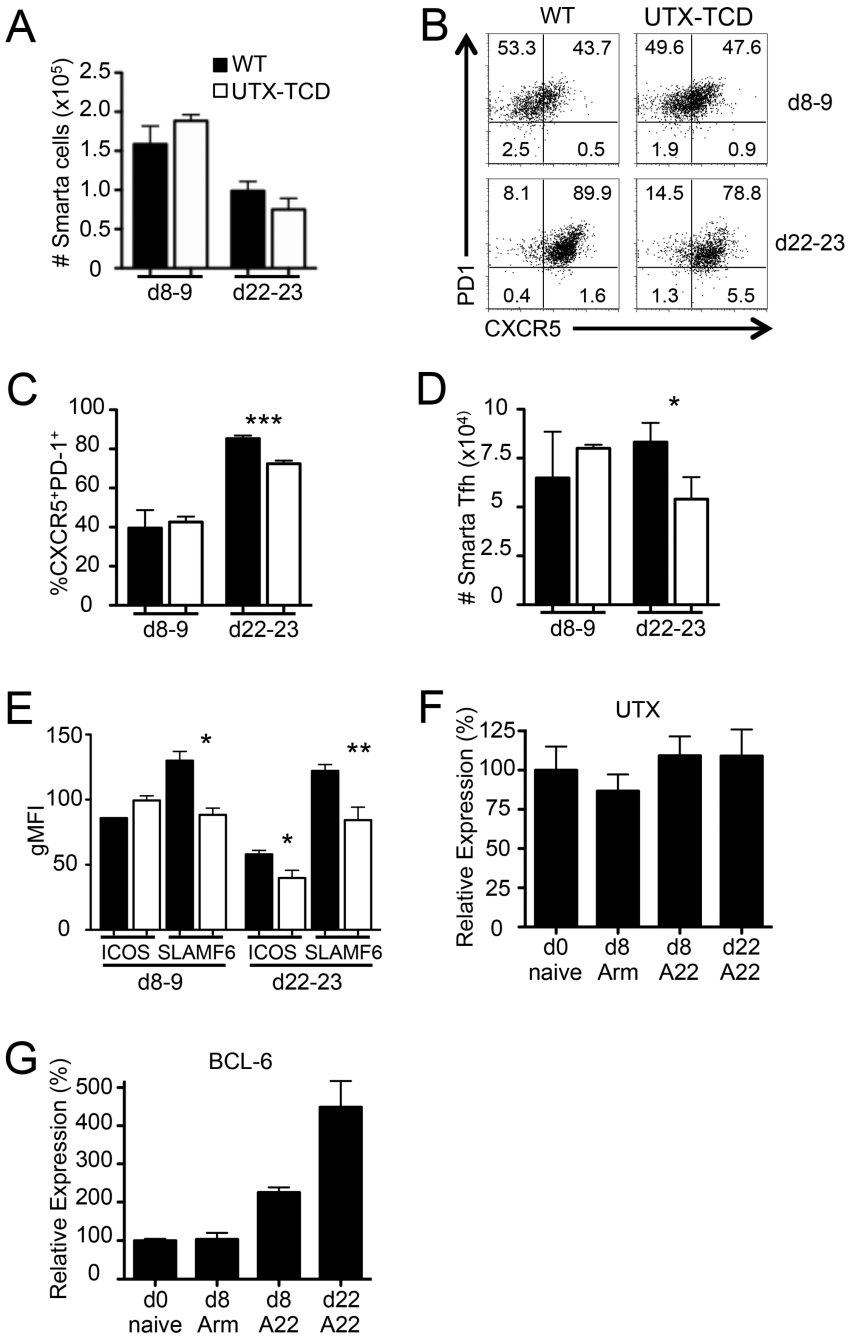

Figure 3. UTX is required for Tfh differentiation during chronic virus infection

WT or UTX-TCD SMARTA $CD4^+$ cells were transferred to C57BL/6 mice followed by infection with LCMV-A22 and analyzed at d8-9 and d22-23 after infection.

(A) The total number of splenic $CD4^+$ $Ly5a^+$ SMARTA cells.

(B) Examples of PD-1 and CXCR5 staining after gating on SMARTA cells.

(C) The frequency of SMARTA cells that are $CXCR5^+PD\text{-}1^+$.

(D) The total number of SMARTA Tfh cells.

(E) The gMFI of ICOS and SLAMF6 on gated $CXCR5^+$ SMARTA cells.

(F) The relative levels of UTX mRNA in WT SMARTA cells as assessed by qRT-PCR and normalized to Actb mRNA.
(G) The relative levels of BCL-6 mRNA in WT SMARTA cells as assessed by qRT-PCR and normalized to Actb mRNA.
All data in this figure are representative of two independent experiments and shown as means + SEM. See also Figure S4 & S5.

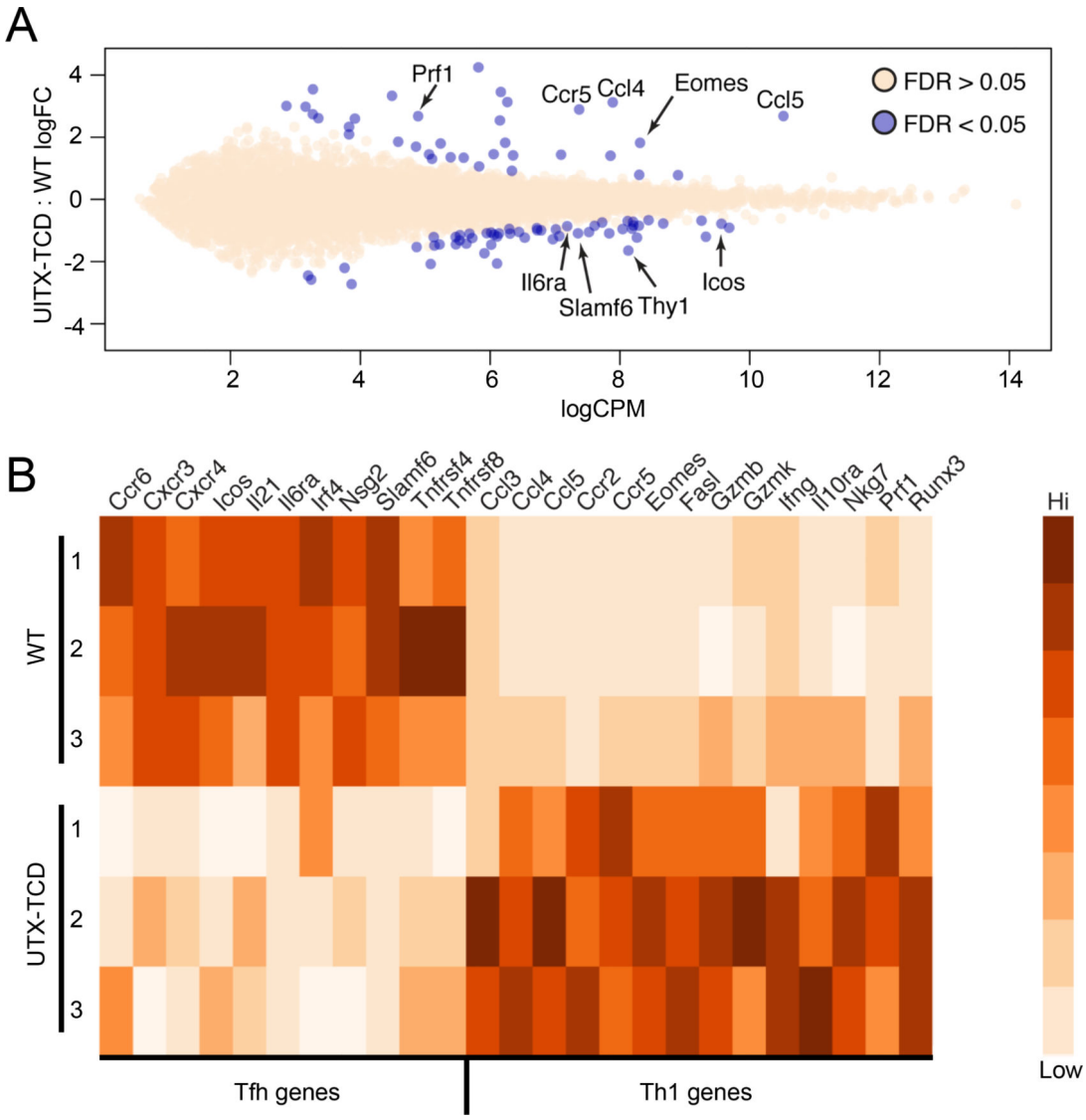

Figure 4. Tfh gene expression is altered in UTX-TCD mice

$CD4^{+}CXCR5^{+}CD62L^{lo}$ T cells were FACS sorted from d21 LCMV-A22 infected spleens. RNA was prepared from 10^{6} cells and subjected to RNA-sequencing.

(A) An EdgeR analysis of RNA-seq data is presented as Log Fold Change (logFC) of UTX-TCD relative to WT plotted against log Counts Per Million reads (logCPM). Significant (FDR<0.05) differences are illustrated as purple circles. Arrows indicate key genes mis-regulated in UTX-TCD cells.

(B) The heat map shows individual replicates of WT and UTX RNA-seq expression of Tfh or Th1 signature genes. Darker red denotes higher expression. Tfh gene expression is reduced in UTX-TCD cells while Th1 gene expression is increased.

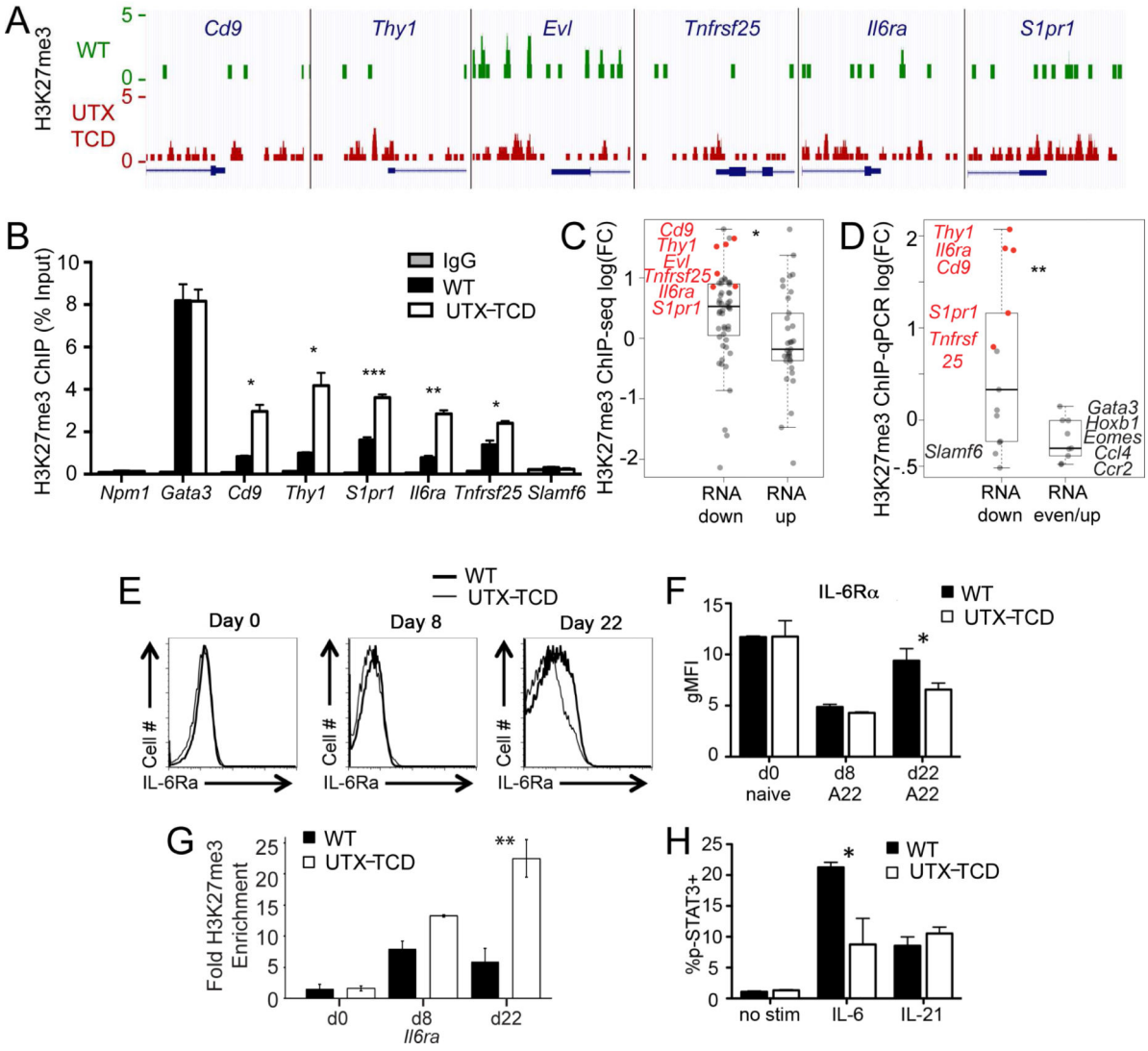

Figure 5. A subset of genes that are misexpressed in UTX-TCD Tfh cells show increased H3K27me3, including *Il6ra*

(A-D) CD4^{+}CXCR5^{+}CD62L^{lo} T cells were FACS sorted from d21 LCMV-A22 infected spleens and subjected to H3K27me3 ChIP-seq or ChIP-qPCR.

(A) UCSC genome browser images of H3K27me3 ChIP-seq tracks from d21 LCMV-A22 infected Tfh at selected promoters demonstrating significant H3K27me3 accumulation in UTX-TCD relative to WT.

(B) H3K27me3 ChIP-qPCR verification of d21 LCMV-A22 CD4^{+}CXCR5^{+}CD62L^{lo} T cells. ChIP was performed with an IgG control (grey) or H3K27me3 ChIP in WT (black) or UTX-TCD cells (white) at indicated genic promoters graphed relative to % input. Npm1 is a negative control locus (active gene) and Gata3 is a positive control (H3K27me3 repressed).

(C) EdgeR analysis of promoter region (transcription start site +/− 1KB) H3K27me3 is presented as Log Fold Change (logFC) of UTX-TCD relative to WT for all genes that were either down-regulated in expression in UTX-TCD (left column) or up-regulated (right column) based on RNA-seq. The logFC is normalized relative to the genome average. All

genes experiencing significant H3K27me3 enrichment in UTX-TCD Tfh are labeled as red dots.

(D) H3K27me3 ChIP-qPCR data was quantified as Log Fold Change (logFC) of UTX-TCD relative to WT for select genes that were either down-regulated in UTX-TCD or up-regulated / unaltered based on RNA-seq analysis. All genes experiencing significant H3K27me3 enrichment in UTX-TCD Tfh are labeled as red dots.

(E-F) $CD4^+$ T cells were FACS sorted from d0 (naïve; $CD62L^{hi}$), day 8 of LCMV-A22 ($CD62L^{lo}$), and day 21 of LCMV-A22 ($CXCR5^+CD62L^{lo}$).

(E) Examples of IL-6Rα staining on WT and UTX-TCD cells at the indicated days.

(F) The gMFI of IL-6Rα on WT and UTX-TCD T cells.

(G) Enrichment of *Il6ra* promoter proximal H3K27me3 by ChIP-qPCR of WT and UTX-TCD cells. Data is graphed as fold H3K27me3 enrichment at *Il6ra* over a control locus lacking H3K27me3 (*Npm1*). .

(H) WT or UTX-TCD SMARTA cells were transferred to WT mice and infected with LCMV-A22 as in Figure 3. Splenocytes were harvested on day 22 pi and cultured with the indicated cytokines for 30 minutes. The percentage of p-STAT3 positive SMARTA cells after the *in vitro* culture.

All data in this figure are representative of at least two independent experiments and shown as means + SEM. See also Figure S6.

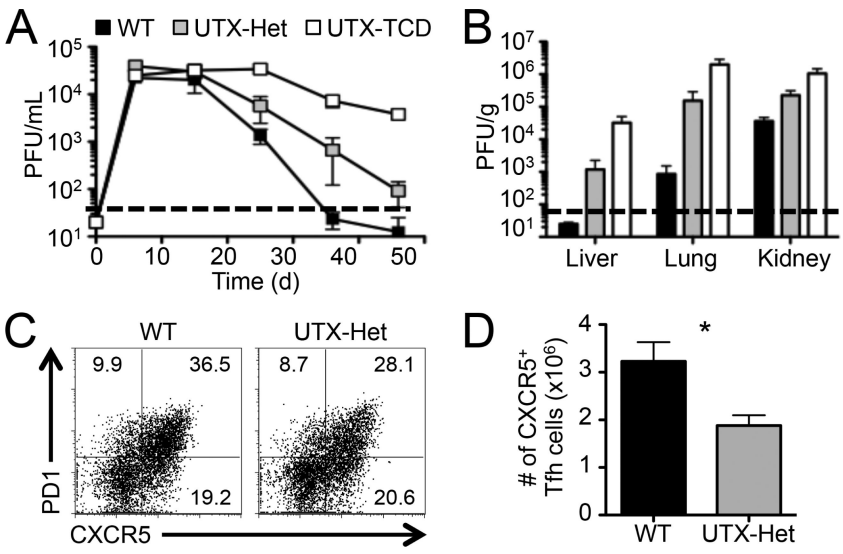

Figure 6. Heterozygous T cell UTX affects virus clearance and Tfh differentiation

WT, UTX-THet, and UTX-TCD mice were infected with LCMV-A22.

(A) The serum viral titer was measured over time.

(B) The level of infectious virus in the indicated tissues at day 55 pi. The dashed lines indicate the level of detection.

(C) Spleens were harvested from WT and UTX-THet mice on day 21 pi and the cells were analyzed by flow cytometry. Examples of PD-1 and CXCR5 staining on gated $CD4^+CD8^-CD19^-$ T cells.

(D) The total number of Tfh Smarta cells ($CXCR5^+PD\text{-}1^+$).

All data in this figure are representative of two independent experiments and shown as means ± SEM.

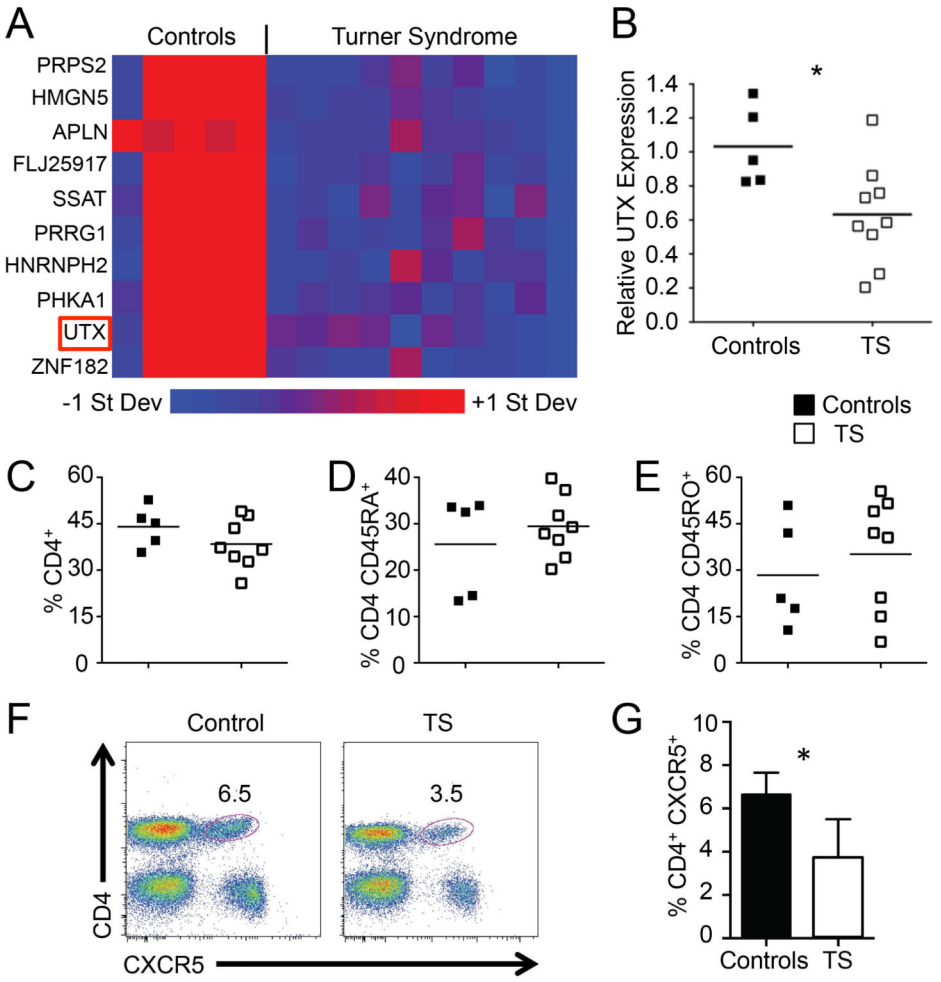

Figure 7. UTX expression is decreased in TS peripheral blood mononuclear cells (PBMCs)

(A) Heat map displaying the relative expression levels of the 10 X-linked genes that are most depressed in Turner Syndrome (TS) subject PBMCs. Expression levels are z-score normalized across rows.

(B) A comparison of array-based UTX expression levels across the subjects. UTX expression was normalized to HPRT in control females and TS subjects by quantitative RT-PCR.

(C) The frequency of $CD4^+$ T cells among all PBMCs. The horizontal bar indicates the mean.

(D) The frequency of $CD45RA^+$ cells among gated $CD4^+$ T cells in the blood. The horizontal bar indicates the mean.

(E) The frequency of $CD45RO^+$ cells among gated $CD4^+$ T cells in the blood. The horizontal bar indicates the mean.

(F) Examples of PBMCs from control of TS subjects that were co-stained for CD4 and CXCR5. The ovals identify the $CD4^+CXCR5^+$ cells; the numbers indicate their frequency among all PBMCs.

(G) The percentage of $CD4^+CXCR5^+$ T cells among all PBMCs. The data is shown as mean + SEM; n=5 for healthy controls, n=7 for TS subjects.

See also Figure S7.